Ensemble of Linear Molecules in Nondispersing Rotational Quantum States: A Molecular Stopwatch

James P. Cryan,[1,2,*] James M. Glownia,[1,3] Douglas W. Broege,[1,3] Yue Ma,[1,3] and Philip H. Bucksbaum[1,2,3]

[1]*PULSE Institute, SLAC National Accelerator Laboratory 2575 Sand Hill Road, Menlo Park, California 94025, USA*

[2]*Department of Physics, Stanford University Stanford, California 94305, USA*

[3]*Department of Applied Physics, Stanford University Stanford, California 94305, USA*

(Received 16 May 2011; published 8 August 2011)

We present a method to create nondispersing rotational quantum states in an ensemble of linear molecules with a well-defined rotational speed in the laboratory frame. Using a sequence of transform-limited laser pulses, we show that these states can be established through a process of rapid adiabatic passage. Coupling between the rotational and pendular motion of the molecules in the laser field can be used to control the detailed angular shape of the rotating ensemble. We describe applications of these rotational states in molecular dissociation and ultrafast metrology.

DOI: 10.1103/PhysRevX.1.011002 Subject Areas: Atomic and Molecular Physics, Chemical Physics, Optics

I. INTRODUCTION

We present a method to create a rotating ensemble of nondispersing quantum rotors based on ideas of strong-field rapid adiabatic passage. The ensemble has $\langle J_z \rangle \neq 0$ and a definite alignment phase angle ϕ, which increases linearly in time like the hands of a clock or a stopwatch.

A linear molecule with an anisotropic polarizability experiences a torque when exposed to a strong laser field [1]. The magnitude and direction of the torque depends on the direction and strength of the incident electric field, and the corresponding pendulum potential can be viewed as an angular trap. We consider the response of an ensemble of such molecules to a pair of copropagating counterrotating circularly polarized laser pulses with a fixed frequency difference. The first pulse in the sequence creates an angular trap with a minimum in the polarization plane, which distorts the ensemble into an oblate distribution [see Fig. 1(c)]. The second pulse turns on before the first pulse turns off, so that the total laser field acquires a slowly rotating linear polarization. The molecules experience a rotating angular trap along the polarization direction, which rotates at half the beat frequency between the two pulses. The rotational speed of the angular trap is fixed, and the trap depth increases with the laser intensity. If the second pulse turns on sufficiently slowly, the ensemble adiabatically follows the eigenstates of the full Hamiltonian. This process adiabatically transforms the planar distribution of molecules into a rotating prolate distribution aligned along the rotating polarization. The quantum mechanical origin of this nondispersing rotation is stimulated Raman couplings among the rotational levels of the molecule, where circularly polarized photons of one rotational handedness are absorbed and the other handedness are stimulated to emit.

The use of strong-field laser pulses to create rotating molecular distributions was first considered in a series of papers on the optical centrifuge [2–4]. The optical centrifuge creates a rotating ensemble by slowly increasing the rotational speed of an angular trap. This process was described semiclassically by Karczmarek [2]. The optical

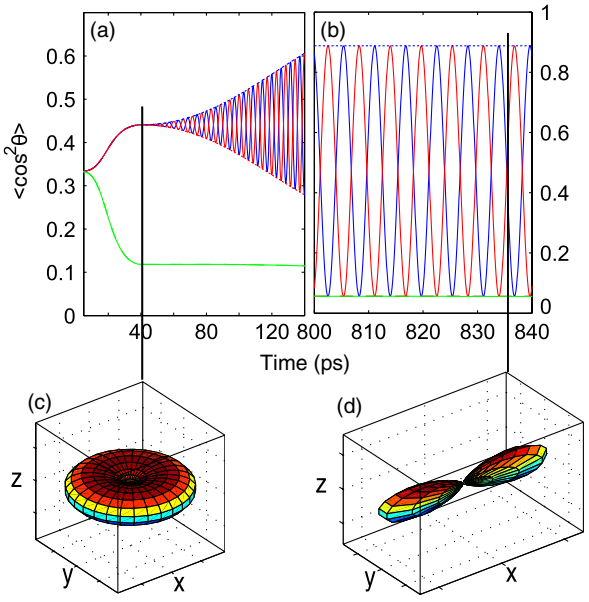

FIG. 1. $\langle \cos^2\theta_x \rangle$ (blue), $\langle \cos^2\theta_y \rangle$ (red), and $\langle \cos^2\theta_z \rangle$ (green) (see text) for (a) short times and (b) long time in the laboratory (solid lines) and the rotating frame (dashed lines). (c) shows the oblate distribution formed by the first pulse at $t = 40$ ps. (d) shows the prolate distribution in the rotating frame at time $t \sim 840$ ps. In (c) and (d), the composite laser field polarization is along the x axis. For this calculation, $\sqrt{\frac{U_0}{I\Omega^2}} = 5.73$, $\Omega = 1.5\frac{B}{\hbar}$, $\tau_1 = 40$ ps, $\tau_2 = 800$ ps.

*jcryan@stanford.edu

centrifuge technique has recently been adapted to use adiabatic passage to create a field-free rotating ensemble which has been called a "cogwheel" state [5]. Rotating molecules are also analogous to Trojan wave packets in Rydberg atoms, first considered by Kalinski [6,7]. The rich dynamics of driven rotor systems has also been recently studied by Topcu and Robicheaux [8].

The analysis here presents many interesting properties of these rotating ensembles that have not been reported for the optical centrifuge. The orientation of the rotating potential maps to the phase difference between the counterrotating laser fields and the rotational speed is directly proportional to the laser frequency difference, so that this system can be used in timing and metrology applications. We present the theory behind the creation of a rotating ensemble and a full density matrix calculation.

II. METHOD

The effective Hamiltonian for a polarizable linear rigid rotor subject to an intense laser pulse of arbitrary polarization is given by

$$H = H_0 + V, \tag{1}$$

where

$$H_0 = BJ^2, \tag{2a}$$

$$V = -\frac{\Delta\alpha}{2}|\vec{E}_\parallel|^2, \tag{2b}$$

and we only include the terms relevant to the dynamics of the rotational state [9]. The angular momentum is quantized along the direction of propagation of the laser pulse, taken as the z axis. H_0 is the field-free rotational Hamiltonian, B is the rotational constant, and V is the potential induced by the laser electric field $\vec{E}$. The differential polarizability of the rotor is $\Delta\alpha = (\alpha_\parallel - \alpha_\perp)$, and $\vec{E}_\parallel$ is the projection of the electric field along the rotor axis. Centrifugal distortion terms are absent since the rotors are rigid.

If we consider two counterrotating circularly polarized fields, the total field is given by

$$\vec{E} = \frac{1}{\sqrt{2}}\{[E_1(t)\cos(\omega_1 t) + E_2(t)\cos(\omega_2 t)]\hat{x} + [E_1(t)\sin(\omega_1 t) - E_2(t)\sin(\omega_2 t)]\hat{y}\}, \tag{3}$$

where $E_i(t)$ is the electric field envelope of each pulse. This equation can be rewritten as:

$$\vec{E} = \vec{E}_\parallel + \vec{E}_\perp = E_x\hat{x} + E_y\hat{y}, \tag{4}$$

$$E_\parallel = \sin\theta(E_x\cos\phi + E_y\sin\phi). \tag{5}$$

Then Eq. (2b) reduces to

$$V = \frac{-\Delta\alpha\sin^2\theta}{2}[(|E_x|^2 - |E_y|^2)\cos^2\phi + |E_y|^2 + 2|E_x||E_y|\cos\phi\sin\phi], \tag{6a}$$

$$|E_x|^2 - |E_y|^2 = |E_1(t)||E_2(t)|\cos(\Delta\omega t), \tag{6b}$$

$$|E_y|^2 = \frac{1}{2}\left[\frac{|E_1(t)|^2}{2} + \frac{|E_2(t)|^2}{2} - |E_1(t)||E_2(t)|\cos(\Delta\omega t)\right], \tag{6c}$$

$$|E_x||E_y| = \tfrac{1}{2}|E_1(t)||E_2(t)|\sin(\Delta\omega t), \tag{6d}$$

where $\Delta\omega = |\omega_1 - \omega_2|$, θ is the polar angle, and ϕ is the azimuthal angle, and again, the z axis is along the propagation direction of the laser field. In Eq. (6) we have integrated over the laser period, leaving only the slow frequency $\Delta\omega$.

It is illustrative to consider the Hamiltonian in a frame rotating with speed $\Omega = \frac{\Delta\omega}{2}$. This is done through a gauge transformation, $U_R = \exp(-il_0\phi/\hbar)$, where $l_0 = I\Omega$ and I is the moment of inertia of the rotor. In this frame the Hamiltonian in Eq. (1) is still appropriate, but there is an additional centrifugal term due to fictitious forces,

$$(H)_R = U_R^\dagger H U_R = BJ^2 + V_R - \Omega J_z = (H_0)_R + V_R, \tag{7}$$

and the induced potential is greatly simplified to resemble a simple pendulum:

$$V_R = \frac{-\Delta\alpha\sin^2\theta}{2}[(|E_x|^2 - |E_y|^2)\cos^2\phi + |E_y|^2], \tag{8a}$$

$$|E_x|^2 - |E_y|^2 = |E_1(t)||E_2(t)|, \tag{8b}$$

$$|E_y|^2 = \frac{1}{2}\left[\frac{E_1(t)^2}{2} + \frac{E_2(t)^2}{2} - |E_1(t)||E_2(t)|\right]. \tag{8c}$$

Again in Eq. (8) we integrate over the laser period.

The Hamiltonian for this system is strikingly similar to that of a Trojan (nonspreading) state first proposed by Kalinski and Eberly [6,7]. The original works on Trojan wave packets in Rydberg atoms considered circularly polarized microwave fields which create a nonspreading state.

We now proceed to calculate the dynamical evolution of the first few eigenvalues and low-lying eigenstates of this system. For ease of calculation we consider only the turn-on of the laser fields. The field envelope functions $E_i(t)$ are $\sin^2$ pulses described by

$$E_1(t) = E_0\left\{[1 - \Theta(t - \tau_1)]\sin^2\left(\frac{\pi t}{2\tau_1}\right) + \Theta(t - \tau_1)\right\}, \tag{9a}$$

$$E_2(t) = E_0\left\{[\Theta(t - \tau_{on}) - \Theta(t - \tau_{on} - \tau_2)]\sin^2\left[\frac{\pi(t - \tau_{on})}{2\tau_2}\right] + \Theta(t - \tau_{on} - \tau_2)\right\}, \tag{9b}$$

where $\Theta(t)$ is the Heaviside step function. We perform calculations in both the laboratory and rotating frames. In either case the full density matrix ρ is propagated using a split operator technique with a ~100 fs step size.

III. RESULTS

The adiabaticity condition for the first pulse is $\tau_1 \gg \frac{h}{2B}$. For the second pulse the adiabaticity condition is more complicated. We find that the turn-on, τ_2, should take place over multiple rotations of the linear field. In addition, τ_2 must also be slow compared to the energy spacing of the pendular states in the rotating frame.

Within a single manifold of states with the same J_z quantum number M, the splitting between states increases linearly with the field strength [10]. However, the splitting between the ground states in different M manifolds decreases with increasing field strength. As the second pulse turns on, the different M manifolds are coupled by the $\sin^2\theta\cos^2\phi$ operator. This means that the spacing between ground states of different M manifolds will determine the adiabatic time scale. In addition to the energy shift caused by the external field, in the rotating frame the energy of each M manifold is shifted by the centrifugal term of the Hamiltonian, Eq. (7). For a given rotational speed, the manifold with M closest to $\frac{\hbar\Omega}{B} - 1$ has a ground state energy near the $M = 0$ manifold ground state energy. Therefore, we find the adiabaticity condition for the second pulse is

$$\tau_2 \gg \frac{h}{\delta(\Omega, E_0) - \hbar K(\Omega)\Omega}, \tag{10}$$

where $\delta(\Omega, E_0)$ is the splitting between the $M = 0$ and $M = K(\Omega) = \mathrm{Int}[\frac{\hbar\Omega}{B} - 1]$ manifolds of the pendular states formed by a circularly polarized field in a nonrotating frame. In this work, $\tau_1 = \tau_{on} = 40$ ps and $\tau_2 = 800$ ps, to satisfy the adiabaticity conditions.

The results of the calculations are shown in Figs. 1–3. These figures show the projection of the ensemble onto the x axis $[\langle\cos^2\theta_x\rangle = \mathrm{Tr}(\rho\sin^2\theta\cos^2\phi)]$, y axis $[\langle\cos^2\theta_y\rangle = \mathrm{Tr}(\rho\sin^2\theta\sin^2\phi)]$, and z axis $[\langle\cos^2\theta_z\rangle = \mathrm{Tr}(\rho\cos^2\theta)]$ in both the rotating and laboratory frames [9]. Figures 1 and 3 also show the calculated probability density of molecules, $|\psi(\theta, \phi)|^2 = \langle\theta, \phi|\rho|\theta, \phi\rangle$ at different times during the pulse sequence.

We find that the degree of alignment along the rotating polarization axis increases linearly with the potential well depth, $U_0 = \frac{\Delta\alpha E_0^2}{2}$, as in the nonrotating, linearly polarized case. The rotational frequency Ω has a more complicated effect on the system: above a critical value of $\Omega \sim \frac{2.5B}{\hbar} = \Omega_{crit}$, there is a marked change in the evolution of the initial state through the adiabatic pulse sequence, which is shown in Fig. 2. The wave function splits and acquires and additional node. The exact value of Ω_{crit} does have a slight dependence on E_0, and the value quoted above is for $\Delta\alpha E_0^2 \sim 74B$.

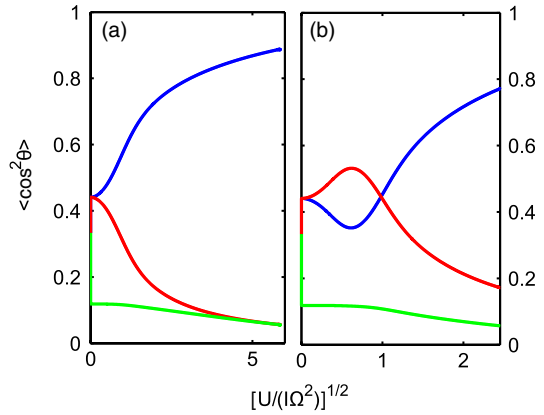

FIG. 2. $\langle\cos^2\theta_x\rangle$ (blue), $\langle\cos^2\theta_y\rangle$ (red), and $\langle\cos^2\theta_z\rangle$ (green) (see text) as a function of $\sqrt{\frac{U}{I\Omega^2}} = \sqrt{\frac{\Delta\alpha|E_1(t)||E_2(t)|}{2I\Omega^2}}$. (a) $\Omega = 1.5\frac{B}{\hbar}$ and (b) $\Omega = 3.5\frac{B}{\hbar}$. In both plots, $\tau_1 = 40$ ps, $\tau_2 = 800$ ps.

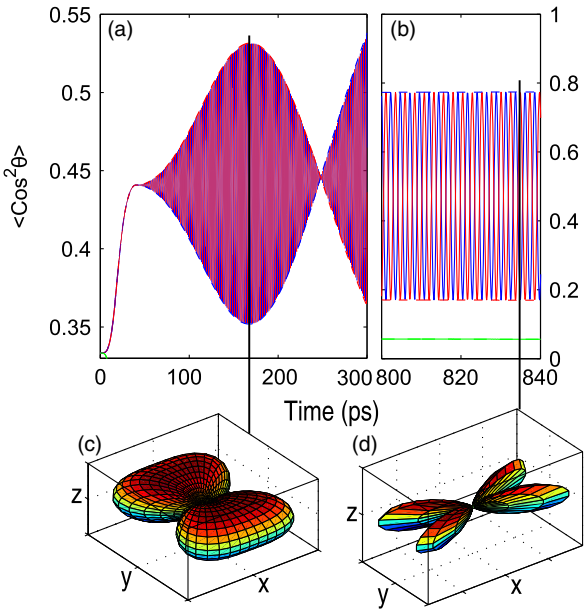

FIG. 3. $\langle\cos^2\theta_x\rangle$ (blue), $\langle\cos^2\theta_y\rangle$ (red), and $\langle\cos^2\theta_z\rangle$ (green) (see text) for (a) short times and (b) long times in the laboratory (solid lines) and the rotating frame (dashed lines). (c) shows the distribution at $t = 165$ ps. (d) shows the prolate distribution in the rotating frame at time $t \sim 840$ ps. In (c) and (d), the composite laser polarization is along the x axis. For this calculation, $\sqrt{\frac{U_0}{I\Omega^2}} = 2.45$, $\Omega = 3.5\frac{B}{\hbar}$, $\tau_1 = 40$ ps, $\tau_2 = 800$ ps.

IV. DISCUSSION

The quantum behavior for $\Omega > \Omega_{crit}$ can be understood by viewing the system in the rotating frame given in Eqs. (7) and (8). To simplify this discussion we will consider the transformation of a pure state, which we can obtain by assuming a rotational temperature of 0 K. Using this simplification, we can now restrict ourselves to only considering states with even values of the quantum

numbers J and M, since the potential V [Eqs. (6) and (8)] only couples states with $\Delta J = 0, \pm 2$, $\Delta M = 0, \pm 2$ [9].

In the rotating frame we can write the Hamiltonian as

$$H_R = H_p - \Omega J_z, \tag{11}$$

where H_p is the pendular Hamiltonian given by

$$H_p = BJ^2 - \frac{\Delta\alpha}{2}\sin^2\theta[E_1(t)E_2(t)\cos^2\phi + |E_y(t)|^2]. \tag{12}$$

We will expand the solution of H_R in the basis of solutions to H_p. Figure 4 shows the diagonal matrix elements of H_R expressed in this basis (the basis of the nonrotating pendular potential). For $\Omega > \Omega_{\text{crit}}$, there is a value of the electric field for which these two matrix elements become degenerate. This degeneracy is lifted in the full Hamiltonian, where the two eigenvalues exhibit an avoided crossing.

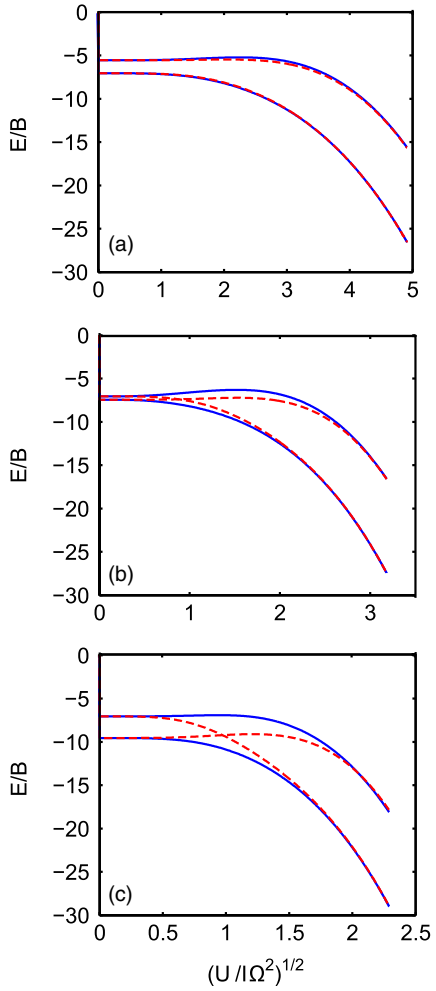

FIG. 4. Diagonal matrix elements of the rotating frame Hamiltonian, H_R Eq. (7), expanded in the basis of eigenstates of the stationary pendulum, H_p Eq. (12) (dashed lines). When the rotating frame Hamiltonian is diagonalizied, the eigenvalues exhibit avoided crossing when $\Omega > \Omega_{\text{crit}}$ (solid lines). $\Omega = 1.75$ (a), 2.7 (b), and 3.75 (c) in units of $\frac{B}{\hbar}$.

In this calculation, all of the molecules start in the ground state of the laboratory frame, $|J = 0, M = 0\rangle$. But, this is not necessarily the ground state of the rotating frame due to the fictitious forces associated with a noninertial reference frame. In fact, when the rotational speed of the trap is above Ω_{crit} the molecules are in the first excited state of the system in the rotational frame prior to the turn-on of the second field. Therefore, an adiabatic transformation will leave the system in the first excited state of the rotational frame Hamiltonian, after passing through the avoided crossing described above. This state has a node in the angular coordinates, which is shown in Fig. 3. Now the structure of the ensembles shown in Figs. 1 and 3 can be clearly understood in terms of the avoided crossings described above.

This result is qualitatively different from the previously reported optical centrifuge, where the system remains in the ground state of the instantaneous rotational frame Hamiltonian due to the adiabatic increase of the angular speed of the trap. However, the method presented here is truly adiabatic, in that if the distribution begins in the ground state of the field-free Hamiltonian in the laboratory frame, then it will be in the ground state of the Hamiltonian which includes the field that is also in the laboratory frame. If $\Omega > \Omega_{\text{crit}}$, then the rotational and laboratory frame ground states are not the same. Also, the sharp nodal features seen here are suppressed at finite temperature, where an incoherent superposition of initial M states effectively fills in the nodes that appear above Ω_{crit}.

In rapid adiabatic passage, the order of operations of adiabatic transformations is important. For the system described in this work, there are two parameters (angular trap depth, U_0, and rotational speed, Ω) which can be varied adiabatically. The difference between the method presented here and the optical centrifuge is in the order of adiabatic transformations. The optical centrifuge first adiabatically increases the angular trap depth and then the rotational speed, which leaves the ensemble in the ground state in the rotating frame. The method presented here starts with a rotating polarization and then slowly changes the rotating angular trap depth. The final state of the system depends on the rotational speed of the trap. In either method, the final parameters of the system are the same, but the final states can be very different. The parameter space is shown in Fig. 5, along with the paths followed by both the optical centrifuge method and the method presented here.

This analysis has focused on the dynamical evolution of the initial state through the pulse sequence to a final state of the system where the magnitude of the two counterrotating fields are equal. If the two pulses have unequal magnitudes, then the total field resembles a slowly rotating linear polarization superposed on a residual circularly polarized

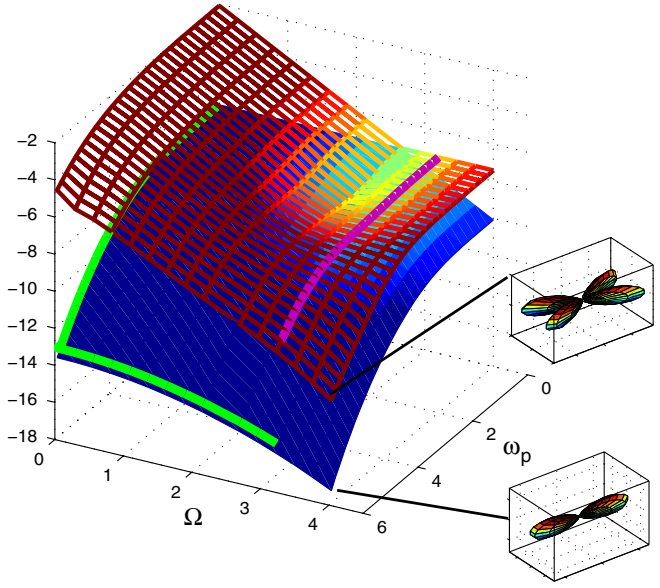

FIG. 5. Energy eignvalues of the rotating frame Hamiltonian, H_R Eq. (7), in units of B, in the (Ω, $\omega_p = \sqrt{\frac{U}{I}}$) parameter space. The x and y axes are in units of $\frac{B}{\hbar}$, and the color of the curve represents the splitting between the eignevalues. Also shown are the paths followed by the optical centrifuge [2] (green) and the method described here (magenta). The insets show $|\psi|^2$ for different points in the parameter space.

field. This type of field creates two angular traps of different strength, one in the θ dimension and one in the ϕ dimension. The dynamic evolution adiabatically follows the ground state of the system throughout the pulse sequence, and we notice an interesting behavior of the ground state of the system when the two fields are unbalanced and $\Omega > \Omega_{\text{crit}}$. Figure 3 clearly shows that for small values of E_2, the ensemble of molecules localizes around the unstable equilibrium point of the classical pendulum. For such small values of E_2, the angular well depth in the ϕ dimension, $U = \frac{\Delta\alpha}{2} E_1(t)E_2(t)$, is much smaller than the centrifugal term ΩJ_z of the Hamiltonian. The presence of this centrifugal term causes a dynamical stabilization of the unstable equilibrium point, but as E_2 grows the stabilization is lost and the ensemble migrates back toward localization around the stable equilibrium point of the classical pendulum.

V. CONCLUSIONS

We have presented a method of strong-field adiabatic control of linear molecules which results in a nondispersing rotational state with $\langle J_z \rangle = I\Omega$. This state can be thought of as rotating at a constant angular speed Ω in the polarization plane.

Adiabatic control of molecular rotational wave packets has already been used to align molecules in the laboratory frame to facilitate molecular frame measurements. [11,12] Nondispersing rotational states expand these techniques to a rotating reference frame. This type of rotating ensemble will allow investigation into the breakdown of the axial recoil approximation. By dissociating the rotating ensemble with a femtosecond probe pulse, the validity of the axial recoil approximation can be tested for various rotational speeds.

In addition, a rotating ensemble could be used as a tool to find the timing between two laser pulses from different sources. In this application, the rotating ensemble could be established using a long pulse (~ 4 ns) infrared laser source. Two other femtosecond laser sources then ionize and dissociate the rotating linear molecules. The dissociation products are collected with a position sensitive detector, and the angular displacement between ion fragments maps directly to the relative time delay between the two pulses. Relative delays could be measured down to $\sim$20 fs resolution, with the appropriate choice of target gas and frequency shift. The nondispersive properties and uniform rotational speed of the molecular state are not dependent on intensity, and so spatial averaging over the laser focus does not destroy these features. The detailed angular distribution does depend on intensity, and, in particular, the bifurcation of the wave packet shown in Fig. 2 will only appear in parts of the focused laser beam where the intensity exceeds a critical threshold. However, if the focal spot size of the probe is much smaller than the adiabatic pump laser, the focal volume averaging effects are minimal.

As a further extrapolation of this technique, we could envision a pulse sequence which uses the optical centrifuge method to move the distribution into the ground state of the rotational frame Hamiltonian, and then turn off the pulse envelopes, while maintaining the constant frequency difference, as in the technique described in this article. The ensemble will now be left in the ground state of the rotational frame field-free Hamiltonian, which is the state $|J = 2, M = 2\rangle$ so long as $\Omega > \Omega_{\text{crit}}$. A subsequent application of the same pulse sequence will return the ensemble to the laboratory ground state, $|J = 0, M = 0\rangle$. Actually the ground state of the rotational frame field-free Hamiltonian changes every time $\Omega = \frac{(J+1)B}{\hbar}$, so by varying the frequency difference of the counterrotating pulses, it should be possible to move the population to any maximal M-state, i.e., $|J, M = J\rangle$, by choosing the appropriate rotational speed.

ACKNOWLEDGMENTS

The authors would like to thank C. Bostedt and R. Coffee for discussions on timing and metrology applications that motivated us to initiate this work, and Y. Silberberg for discussions on adiabatic passage. This research is supported through the PULSE Institute at the SLAC National Accelerator Laboratory by the U.S. Department of Energy, Office of Basic Energy Science.

[1] H. Stapelfeldt and T. Seideman, *Colloquium: Aligning Molecules with Strong Laser Pulses*, Rev. Mod. Phys. **75**, 543 (2003).

[2] J. Karczmarek, J. Wright, P. Corkum, and M. Ivanov, *Optical Centrifuge for Molecules*, Phys. Rev. Lett. **82**, 3420 (1999).

[3] D. M. Villeneuve, S. A. Aseyev, P. Dietrich, M. Spanner, M. Y. Ivanov, and P. B. Corkum, *Forced Molecular Rotation in an Optical Centrifuge*, Phys. Rev. Lett. **85**, 542 (2000).

[4] M. Spanner, K. M. Davitt, and M. Y. Ivanov, *Stability of Angular Confinement and Rotational Acceleration of a Diatomic Molecule in an Optical Centrifuge*, J. Chem. Phys. **115**, 8403 (2001).

[5] M. Lapert, S. Guérin, and D. Sugny, *Field-Free Quantum Cogwheel by Shaping of Rotational Wave Packets*, Phys. Rev. A **83**, 013403 (2011).

[6] M. Kalinski and J. H. Eberly, *New States of Hydrogen in a Circularly Polarized Electromagnetic Field*, Phys. Rev. Lett. **77**, 2420 (1996).

[7] M. Kalinski and J. H. Eberly, *Trojan Wave Packets: Mathieu Theory and Generation from Circular States*, Phys. Rev. A **53**, 1715 (1996).

[8] T. Topcu and F. Robicheaux, *Multiphoton Population Transfer in Systems Violating the Classical Twist Condition: A Comparative Study of Separatrix Crossing in Phase Space*, Phys. Rev. E **83**, 046607 (2011).

[9] D. Daems, S. Guérin, E. Hertz, H. R. Jauslin, B. Lavorel, and O. Faucher, *Field-Free Two-Direction Alignment Alternation of Linear Molecules by Elliptic Laser Pulses*, Phys. Rev. Lett. **95**, 063005 (2005).

[10] B. Friedrich and D. Herschbach, *Alignment and Trapping of Molecules in Intense Laser Fields*, Phys. Rev. Lett. **74**, 4623 (1995).

[11] L. Holmegaard, J. L. Hansen, L. Kalhoj, S. L. Kragh, H. Stapelfeldt, F. Filsinger, J. Kupper, G. Meijer, D. Dimitrovski, and M. Abu-samha *et al.*, *Photoelectron Angular Distributions from Strong-Field Ionization of Oriented Molecules*, Nature Phys. **6**, 428 (2010).

[12] J. L. Hansen, H. Stapelfeldt, D. Dimitrovski, M. Abu-samha, C. P. J. Martiny, and L. B. Madsen, *Time-Resolved Photoelectron Angular Distributions from Strong-Field Ionization of Rotating Naphthalene Molecules*, Phys. Rev. Lett. **106**, 073001 (2011).